Otolaryngology Articles   Otolaryngology - Head and Neck Surgery

3-12-2021

MicroRNA Profile Differentiates Head and Neck Keloid and Adjacent Normal Skin Tissue

Lamont R. Jones
Henry Ford Health, ljones5@hfhs.org

Albert M. Levin
Henry Ford Health, alevin1@hfhs.org

Xiangguo Dai
Henry Ford Health, XDAI1@hfhs.org

Indrani Datta
Henry Ford Health, idatta1@hfhs.org

Jia Li
Henry Ford Health, jli4@hfhs.org

See next page for additional authors

Follow this and additional works at: https://scholarlycommons.henryford.com/otolaryngology_articles

Authors

Lamont R. Jones, Albert M. Levin, Xiangguo Dai, Indrani Datta, Jia Li, Congcong Yin, and Qing-Sheng Mi

MicroRNA Profile Differentiates Head and Neck Keloid and Adjacent Normal Skin Tissue

Lamont R. Jones, MD, MBA,[1] Albert M. Levin, PhD,[2,3] Xiangguo Dai, PhD,[1] Indrani Datta, MS,[2,3] Jia Li, PhD,[2,3] Congcong Yin, MD, PhD,[4] and Qing-Sheng Mi, MD, PhD[4]

Keloid research and treatment are hindered by the lack of keloid-specific biomarkers. Matched normal skin is an important control to eliminate confounding. However, although clinically normal and accessible, there are concerns about the use of either distant donor sites because of the risk of keloid development or the adjacent tissue, as it may harbor keloid tissue. A biomarker that distinguishes keloid and adjacent normal tissue would address these concerns and provide a molecular standard that would improve comparability across keloid research studies. Recently, there has been a shift toward a deeper characterization of epigenetic modifications to better understand keloid pathogenesis.[1] Because of their specificity and ability to modulate gene expression, microRNAs (miRNAs) are one such class of epigenetic modifiers that could be utilized as a functional molecular biomarker of keloids given that miRNAs are known to influence keloids[2]. Therefore, we sought to identify miRNA able to differentiate keloid and adjacent normal tissue.

Fresh, primary, and untreated head and neck (H&N) keloid and adjacent matched normal skin were obtained through an approved IRB protocol. Adjacent normal skin was determined clinically. Discovery and validation cohorts were composed of 15 and 7 patients, respectively (Table 1). Total RNA was extracted, using the Ambion RiboPure™ kit. The TaqMan® MiRNA array (card A & B), which profiles 752 miRNAs, was used to determine miRNA expression in terms of negative Delta Cycle Threshold values. Global mean normalization was used to standardize miRNA measurements across discovery cohort patients. TaqMan Advanced miRNA real-time polymerase chain reaction assays were used to validate differentially expressed miRNAs (DEMs), in the validation cohort.

Univariate analysis was performed on the discovery cohort, using linear regression models fit using generalized estimating equations to account for the paired nature of the specimens. To account for multiple testing, significant DEMs were identified at a false discovery rate (FDR) of 0.05.[3] Next, a panel of miRNAs was selected to identify a multi-miRNA profile that best predicted the keloid diagnosis. We deployed a strategy of feature selection based on the univariate analysis refined with a minimum twofold change difference and detectable in ≥80% of the specimens, followed by multivariable modeling to maximize sensitivity and specificity. The multivariable prediction methods evaluated were support vector machine (SVM) and random forest (RF). Model selection was performed in the discovery cohort using a two-layer fivefold cross-validation scheme.[4] The inner layer identified the optimal number of miRNAs and the outer layer measured model performance based on the area under the receiver operator characteristic curve (AUC). The individual DEMs and the accuracy of the RF- and SVM-based multi-miRNA biomarkers were evaluated in the validation cohort. To gain functional insights into the DEMs, target gene analysis was performed using Qiagen's microRNA Target filter in Ingenuity Pathway Analysis (IPA) (QIAGEN, Inc.).

Departments of ¹Otolaryngology and ²Public Health, Henry Ford Health System, Detroit, Michigan, USA.
³Center for Bioinformatics, Henry Ford Health System, Detroit, Michigan, USA.
⁴Department of Dermatology, Henry Ford Health System, Detroit, Michigan, USA.
The study was approved by the Henry Ford Health System IRB committee.

*Address correspondence to: Lamont R. Jones, MD, MBA, Department of Otolaryngology, Henry Ford Health System, 2799 West Grand Boulevard, Detroit, MI 48202, USA, Email: ljones5@hfhs.org or Qing-Sheng Mi, MD, PhD, 2799 West Grand Boulevard Detroit, MI 48202, USA, Email: qmi1@hfhs.org

Table 1. Test and validation cohorts

Cohort	Age	Gender	Race	Location
Discovery				
1	86	M	CA	Neck
2	25	F	AA	Ear
3	28	F	CA	Ear
4	23	M	AA	Ear
5	21	F	CA	Ear
6	46	F	AA	Neck
7	21	F	CA	Ear
8	52	M	AA	Cheek
9	15	F	AA	Ear
10	32	M	AA	Ear
11	33	M	AA	Ear
12	87	F	AA	Ear
13	51	F	AA	Postauricular
14	17	M	AA	Ear
15	19	M	AA	Ear
Validation				
1	31	M	AA	Ear
2	30	M	AA	Neck
3	20	F	AA	Ear
4	21	M	AA	Ear
5	22	F	AA	Ear
6	21	F	HA	Ear
7	29	F	AA	Ear

AA, African American; CA, Caucasian American; HA, Hispanic American.

Table 2. Differentially expressed microRNA in keloid compared to matched normal tissue

	Test cohort		Validation cohort	
DEM	Adjusted p value	FC K:N	Adjusted p value	FC K:N
hsa-miR-127-3p	<1.0E-16	2.32	1.14E-3	2.82
hsa-miR-424-3p	<1.0E-16	3.72	3.57E-3	5.13
hsa-miR-377-3p	<1.0E-16	2.17	1.08E-3	4.11
hsa-miR-382-5p	<1.0E-16	3.21	1.41E-3	3.66
hsa-miR-503-5p	1.11E-16	3.16	2.02E-4	4.35
hsa-miR-154-5p	8.88E-16	2.17	1.6E-4	1.87
hsa-miR-323a-3p[a]	1.11E-15	3.54	7.48E-4	4.59
hsa-miR-652-3p[a]	2.00E-15	−3.15	1.41E-3	−3.45
hsa-miR-494-3p[a]	2.00E-15	3.17	2.86E-05	3.81
hsa-miR-424-5p	1.65E-13	2.33	1.6E-4	5.01
hsa-miR-485-3p[a]	7.21E-13	2.55	01.31E-2	3.30
hsa-miR-134-5p	6.61E-10	2.42	7.48E-4	3.27
hsa-miR-487b-3p[a]	7.89E-10	3.21	2.39E-2	4.10
hsa-miR-429	1.53E-09	−3.97	0.948	0.277
hsa-miR-31-5p	3.23E-08	2.72	0.011	3.56
hsa-miR-378a-3p[a]	3.57E-08	−4.02	0.043	−1.22
hsa-miR-1291[a]	3.04E-07	−2.36	0.384	−1.01

[a]Novel to keloids.
FC, fold change; K, keloid; N, normal.

Univariate analysis identified 140 DEMs at an FDR <0.05. The cross-validation scheme identified 16 and 17 of the DEMs as the optimal number of miRNA for the respective SVM and RF classifiers (Table 2). Both models demonstrated a high degree of differentiation (SVM AUC = 0.969, RF AUC = 0.997; Fig. 1). In the validation cohort, all but one DEM was validated, and both the RF and SVM classification models achieved AUCs of 1.00 in the validation cohort (Fig. 1). Thirteen of the DEMs were upregulated in keloids (Table 2). The top 10 diseases and biofunctions and networks identified by IPA are listed in Supplementary Figure S1.

Of the 17 H&N keloid-specific DEMs, 10 previously reported in the keloid literature (Table 2), including mir-134-5p, mir-127-3p, mir-31-5p, mir-424-3p, mir-424-5p, mir-382-5p, mir-377-3p, mir-503-5p, and mir-429, which also had similar expression profiles. Target gene analysis support a link between the DEMs and keloid pathogenesis because of their predicted and experimentally validated interactions with canonical pathways such as transforming growth factor-β (TGF-β) and Wnt/β-catenin signaling (Supplementary Table S1).

The seven DEMs not previously reported in the literature offer new insights into keloid pathogenesis. For example, mir-323a-3p targets TGF-β and TGF-α, and its overexpression suppresses lung fibrosis.[5] mir-1291, a tumor suppressor,[6] regulates epithelial mesenchymal transition and fibrosis in endometriosis[7]. These findings suggest potential roles for mir-323a-3p and mir-1291 in the keloid tissue microenvironment.

Diagnostic biomarkers that simultaneously identify keloid and distinguish normal skin define a precise molecular phenotype to improve consistency on keloid definition across studies, could provide further insight into keloid pathogenesis, and identify novel keloid therapeutic targets. In our study, we identified and validated DEMs able to distinguish keloid and adjacent normal skin from the H&N. The findings are noteworthy as this is the first reported diagnostic biomarker profile specific to keloids. Nevertheless, the results should be validated in larger cohorts of patients and the functional significance of the component miRNA should be further explored.

Authors' Contributions

All authors contributed to the study design, the acquisition, analysis, and interpretation of results. Drs. L.R.J., Q.-S.M., I.D., and A.M.L. were responsible for drafting and editing the article. All authors reviewed and approved the final article before submission.

Author Disclosure Statement

No competing financial interests exist.

Supplementary Material
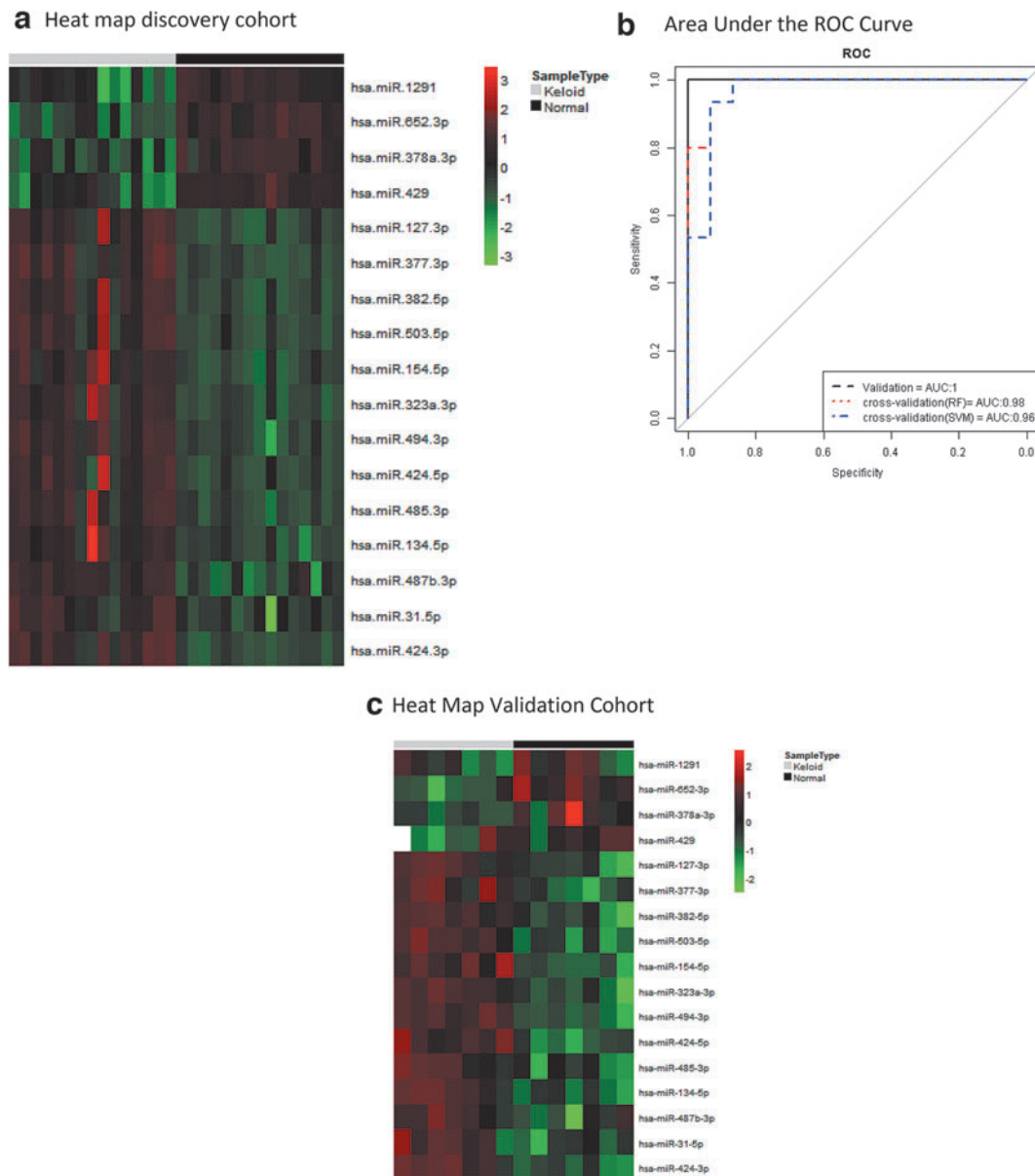
Supplementary Figure S1
Supplementary Table S1

Fig. 1. **(a)** Heat map showing the tissue expression level of 17 differentially expressed miRNAs in keloids with matched normal skin controls in training data. **(b)** A panel of miRNAs that best discriminate keloids from matched normal skin controls based on the RF and SVM analysis. ROC analysis discriminates keloid from matched controls using fivefold cross-validation and independent validation. The estimated AUC is 0.98 using RF and AUC is 0.96 using SVM in fivefold cross-validation. AUC is 1 on independent validation data. **(c)** Heat map showing the tissue expression level of 17 differentially expressed miRNAs in keloids with matched normal skin controls in independent validation data. AUC, area under the curve; miRNA, microRNA; RF, random forest; ROC, receiver operating characteristics; SVM, support vector machine.

References

1. He Y, Deng Z, Alghamdi M, Lu L, Fear MW, He L. From genetics to epigenetics: new insights into keloid scarring. *Cell Prolif.* 2017;50:e12326.
2. Liu Y, Yang D, Xiao Z, Zhang M. Mirna expression profiles in keloid tissue and corresponding normal skin tissue. *Aesthetic Plast Surg.* 2012;36:193–201.
3. Benjamini Y, Drai D, Elmer G, Kafkafi N, Golani I. Controlling the false discovery rate in behavior genetics research. *Behav Brain Res.* 2001;125:279–284.
4. Balasubramanian V, Ho S-S, Vovk V. *Conformal Prediction for Reliable Machine Learning: Theory, Adaptations, and Applications.*
Amsterdam; Boston: Elsevier/Morgan Kaufmann; 2014; p. xxiii, 298 pages.
5. Ge L, Habiel DM, Hansbro PM, et al. Mir-323a-3p regulates lung fibrosis by targeting multiple profibrotic pathways. *JCI Insight.* 2016;1:e90301.
6. Yamasaki T, Seki N, Yoshino H, et al. Tumor-suppressive microrna-1291 directly regulates glucose transporter 1 in renal cell carcinoma. *Cancer Sci.* 2013;104:1411–1419.
7. Xu Q, Duan H, Gan L, et al. Microrna-1291 promotes endometrial fibrosis by regulating the arhgap29-rhoa/rock1 signaling pathway in a murine model. *Mol Med Rep.* 2017;16:4501–4510.